INFORMATICS JOURNALS

Research Article

Journal of Natural Remedies
DOI: 10.18311/jnr/2026/54543

eISSN: 2320-3358 | Vol 26(3), 2026 | pp. 000-000

In Silico Evaluation of Anti-diabetic and Immunomodulatory Activities of Phytoconstituents from *Lepidagathen pungens* and *Capparis grandis*

C. Nagamani[1] and P. Balaji[2*]

[1]Department of Pharmaceutical Chemistry, School of Pharmaceutical Sciences, VISTAS, Pallavaram, Chennai – 600117, Tamil Nadu, India

[2]Department of Pharmacology, School of Pharmaceutical Sciences, VISTAS, Pallavaram, Chennai – 600117, Tamil Nadu, India; pharmacology.balaji@gmail.com

Abstract

Background: Diabetes mellitus is strongly associated with oxidative stress and immunological dysfunction, exacerbating metabolic and inflammatory challenges. Therapeutic compounds produced from bioactive plant molecules have garnered significant interest due to their extensive impact on various biological targets. **Aim:** This study employed molecular docking and *in vitro* antioxidant assays to assess the antioxidant, immunomodulatory, and anti-diabetic activities of bioactive compounds derived from *Capparis grandis* and *Lepidagathen pungens*. **Methods:** To elucidate the interactions between Cristatin-A from *L. pungens* and Cappariloside from *C. grandis* with two target proteins, Human Collagenase-3 (MMP-13) and the c-Src SH3 domain mutant T125S, we performed a molecular docking study with Molegro Virtual Docker (MVD). These proteins are involved in pathways that govern metabolism and the immune system. We examined its docking efficacy with two reference medications, Glibenclamide and Azathioprine. We employed tests to evaluate the scavenging of hydroxyl radicals, superoxide radicals, and lipid peroxidation to ascertain the efficacy of the hydro-alcoholic extract of *C. grandis* (HAECG) against free radicals. **Results:** Cristatin-A and Cappariloside demonstrated robust hydrogen bond interactions with both target proteins and achieved favourable MolDock scores in docking assessments. This signifies that their binding affinity surpasses that of the reference medications. These interactions indicate the potential for a dual role in modulating the immune system and glycemic control. The IC_{50} values of 22.21 µg/mL for hydroxyl radicals and 22.04 µg/mL for superoxide radicals demonstrate that HAECG displayed considerable radical scavenging activity in antioxidant assessments. Consistent with standard treatment, the extract suppressed lipid peroxidation, exhibiting an IC_{50} value of 27.618 µg/mL. **Conclusion:** The data indicate that *C. grandis* and *L. pungens* are abundant in bioactive chemicals with potential antioxidant, immunomodulatory, and anti-diabetic effects. These plants may yield potential novel plant-based therapeutics for metabolic and immune system disorders.

Major Findings: In comparison to conventional pharmaceuticals, Cristatin-A and Cappariloside received superior docking scores owing to their robust binding affinity for MMP-13 and c-Src SH3 domain proteins. The hydro-alcoholic extract of *C. grandis* shows considerable antioxidant activity, perhaps aiding in the management of oxidative stress linked to diabetes and immune system problems.

Keywords: Anti-diabetic Activity, *Capparis grandis,* Immunomodulation, *Lepidagathen pungens,* Molecular Docking

(Article Chronicle: Article Received on: 23.05.2025; Revised on: 09.01.2026; Accepted on: 22.01.2026)

1. Introduction

Diabetes mellitus is a chronic metabolic disease that is defined by unremitting hyperglycemia caused by malfunctions in the secretion of insulin, the insulin activity, or both. It is among the major health problems in the world that, through its complications, results in high levels of morbidity and mortality through neuropathy,

*Author for correspondence

nephropathy, and cardiovascular diseases[1,2]. These progressive courses of the disease and the weaknesses of current treatment options have prompted the pursuit of new treatment agents, especially those based on natural sources, as they have multi-targeted effects and fewer side effects. Herbal medicines have been known to have the potential of restoring glucose homeostasis along various mechanisms that include increasing insulin secretion, improving the peripheral uptake of glucose, and inhibiting carbohydrate-digesting enzymes[3-5].

Simultaneously, the immune system is crucial in the development and progression of diabetes, particularly in autoimmune diseases such as type 1 diabetes and in the chronic low-grade inflammation of type 2 diabetes. Immunomodulation has consequently become one of the most important treatment interventions in the management of diabetes, as it helps to restore balance in the immune system and stops the destruction of 2-cells. The herbal immunomodulators contain bioactive compounds that help control the immune response by regulating cytokine production, macrophage activity, and balancing Th1/Th2 immune activities[6-8].

Lepidagathen pungens and *Capparis grandis* are two of the most promising medicinal plants with promising phytochemical profiles in the effort to treat metabolic and inflammatory diseases in the traditional therapeutic approach. Individual constituents of these plants, including flavonoids, alkaloids, and phenolic compounds, have high antioxidant, anti-diabetic, and immunomodulatory effects. The investigation of the synergistic action of such phytoconstituents can help produce plant-based therapeutic agents to treat diabetes in its entirety through the control of glycemic and immune responses[9,10].

2. Materials and Methods

2.1 Network Pharmacology

The active phytoconstituents of *C. grandis* and *L. pungens* were identified through a literature review conducted in this *in-silico* network pharmacology study. Based on the Swiss Target Prediction database, these phytoconstituents were then analysed to determine their disease targets. The Gene Cards database was used to find potential targets for Diabetes and Immunomodulation. To identify the common targets between phytoconstituents and diseases, a Venn diagram was generated using Venny 2.1.0 software. Based on the STRING database, the common targets were further analysed by constructing a Protein-Protein Interaction (PPI) network with a confidence score threshold of ≥ 0.4. In order to further analyse enrichment, this network was imported into Cytoscape 3.10.3. Using the Maximal Clique Centrality (MCC) method, the top ten hub targets were ranked. A molecular docking study was conducted on the target with the highest ranking to evaluate potential interactions with phytoconstituents. The Swiss Target Prediction server was used to predict targets for *C. grandis* and *L. pungens* using canonical SMILES obtained from the PubChem database. An analysis of the overlap between the predicted targets of phytoconstituents and diabetic and immunomodulation targets was also conducted using a Venn diagram in order to determine which targets are most relevant to further study. Finally, molecular docking studies, hub identification, and data visualisation were used to interpret the PPI network[11-13].

2.2 Molecular Docking

2.2.1 Protein Preparation

The docking experiment was started with the preparation of the target protein structures in MVD. The Protein Data Bank was searched with three-dimensional crystal structures of the Human Collagenase 3 (MMP-13) with the PDB ID: 4G0D and Intertwined Dimer of the c-Src SH3 Domain Mutant (T125S) with PDB ID: 7A3D. Both proteins were selected according to their high-resolution data (less than 2.5 A) without error due to accuracy and structural integrity. The individual proteins were each imported into the MVD workspace via File Import Molecule Protein, and structural refinement and optimisation were done. The water molecules had been filtered out, except when necessary, in stabilising the ligand, and non-essential heteroatoms had been eliminated in favour of eliminating co-crystallised ligands and irrelevant chains, which could cause interference during docking. The Repair Add Missing Hydrogens tool was used to add polar hydrogens in order to provide proper charge distribution and geometry. The MVD automatically attached the correct atom types and bond orders to ensure that there was consistency in molecules. The Detect Cavities function was then used to detect possible binding sites in each protein.

The active binding pocket to be further simulated was the most biologically relevant cavity, which has the best volume and less energy[12-15].

2.2.2 Ligand Preparation

Ligand preparation is an important part of the molecular docking procedure in order to predict the interaction with the target proteins in an acceptable manner. In this work, the PubChem database was searched to obtain different bioactive ligands according to an investigation of the literature on phytochemical constituents of *L. pungens* and *C. grandis*. Chemical structures of the chosen compounds were received in 2D or 3D format and stored in standard file types like mol or sdf to be used further. The minimisation of the energy of each ligand was conducted with the help of the Chem3D software, through the application of the MM2 or MMFF94 force field to obtain a geometrically stable and energetically favourable conformation. This was an effective step in minimising steric strain and maximising bond angles, as well as making sure that the ligands assumed their lowest energy formations. Minimised 3D structures were then exported as moles2 or SDF structures to be compatible with Molegro Virtual Docker (MVD). Importation of the ligands into MVD occurred through File Import Molecule Ligand, and valence requirements were met by adding missing hydrogen atoms. The software automatically checked and corrected values of atom types and bond orders. In case of need, the structures were turned into 3D conformers, making them fully ready to properly docking simulations and interaction analysis[16,17].

2.2.3 Molecular Import and Preparation

Both the target proteins of interest, Human Collagenase 3 (MMP-13, PDB ID: 4G0D) and the Intertwined Dimer of the c-Src SH3 Domain Mutant T125S (PDB ID: 7A3D), along with the chosen ligands of *L. pungens* and C. grandi, were imported into the MVD workspace before the docking process was started in MVD. The successful visualisation of the two molecules ratified adequate organisation and preparedness to examine the interaction. The protonation state of both proteins and ligands was confirmed to match the physiological pH (~7.4), because incorrect protonation will cause false electrostatic potentials and hydrogen-bonding patterns, and unreliable results with docking. All the molecules were properly hydrogenated and charged to give realistic molecular simulations. After this step to secure the structural integrity, the binding sites were defined with the help of the Docking Wizard tool (Select Protein Define Binding Site). The active cavities previously identified were used as docking sites; although they were not automatically identified, they were typically established manually by specifying the centre coordinates (X, Y, Z) and radius (812 A) to cover the active region. This step made sure that the docking algorithm targeted the biological interests of the target proteins with high accuracy in predicting ligand interactions[18-20].

2.3 Docking Setup

In Molegro Virtual Docker, Docking Wizard, a systematic interface that facilitated the configuration and execution of the docking simulations was initiated. Docking: A new docking project was generated under Docking → Start Docking Wizard → Create New Docking Job. In order to achieve the highest accuracy and reproducibility, a single algorithm, MolDock SE (Simplex Evolution), was chosen because of its high proficiency in searching the ligand conformational space. The scoring function was to be the MolDock Score or Re-Rank Score, which determines the binding affinity on the basis of non-bonded interactions and steric complementarity. The parameters in the simulation were changed based on the complexity of the system: number of runs = 10-30, max iteration = 1500-2000 and population size = 50-100. To increase accuracy, Constrain Docking was enabled, where the residues of certain amino acids were to interact with a ligand. The energy threshold was pegged at 100, and a limit of 10-20 poses was saved on each ligand to simplify the analysis. After everything was set, docking was run by clicking Start Docking, which gave the software the capacity to run iterative conformational searches until the optimum binding pose converged to the lowest conceivable energy scores[21-23].

2.4 Docking Analysis

Once the docking runs were complete, MVD produced a prioritised list of ligand protein binding poses with MolDock Scores, which are predicted binding energies. The score with the lowest (most negative) corresponded to the most stable and energetically

efficient complex, which implies a high affinity of the ligand with the protein active site. In order to visualise molecular interactions, the View Ligand Interactions option was used, which gives a detailed visualisation of hydrogen bonds, hydrophobic contacts, and electrostatic interactions between ligands of *L. pungens* and *C. grandis* and residues of MMP-13 and c-Src SH3 proteins. Parameters of interaction, including bond length (in A) and interacting amino acids, were examined to determine stability and specificity. The posed ligands were docked when possible and compared with the co-crystallised ligands to validate the accuracy. Also, the components of energy, such as hydrogen bonding, van der Waals, steric, electrostatic and torsional penalties, were tested individually in order to clarify the mechanism of binding. This was exported to final results, either in mol2, PDB or image (File → Export Results). The obtained 2D interaction maps have also been utilised to prepare the figures and document the publications[24-27].

2.5 *In Vitro* Antioxidant Assay

2.5.1 Superoxide Radical Scavenging Activity

This method is used to determine the effectiveness of superoxide radical scavenging by using nitro blue tetrazolium (NBT) [21]. PMS/NADH is a non-enzymatic process that generates superoxide radicals that reduce NBT to the purple colour formazan in the assay. The extract contained phosphate buffer (0.5 mL, 100mM, pH 7.4), 1.0 mL of NADH (0.4mM), 1.0 mL of NBT (0.156mM), 0.1 mL of PMS (0.06mM) and 3 mL of the Extract/standard drugs (Ascorbic acid) of various concentrations (10- 50 µg/mL, in 90% ethanol). An appropriate blank was used to determine the quantity of formazan produced after the reaction mixture was incubated at 25 °C for 1h[26-28].

2.5.2 Hydroxyl Radical Scavenging Activity

The extract contained 0.1 mL of 2-deoxy-2-ribose (10mM), 0.33mL of phosphate buffer (50mM, pH 7.4), 0.1 mL of $FeCl_3$ (0.1 mM), 0.1 mlethylene-diamine tetra-acetic acid (EDTA) (0.1mM), 0.1 mL of H_2O_2 (mM), 0.1 mL of ascorbic acid (1mM) and 1.0 mL of various concentrations (5-50 µg/mL) of the Extract/standards (Ascorbic acid). 1.0 mL of 2.8% (v/v) TCA was added to the reaction mix after 45 min at 37 °C, along with 1.0 mL of [thiobarbituric acid, TBA, 0.5% (v/v) in 0.025 mol/L NaOH solution containing 0.2% (w/v) butylated hydroxyl anisole, BHA], and a 15 min incubation at 95 °C developed the pink chromogen. After cooling, the absorbance was measured at 532 nm with a blank solution[29,30].

2.5.3 Lipid Peroxidation Scavenging Activity

Extract (0.1 mL, 25% w/v) in Tris-HCl buffer (40 mM, pH 7.0), KCl (30 mM), $FeCl_3$ (0.16 mM) and ascorbic acid (0.06 mM) was incubated for 1 h at 37 °C at various concentrations (50- 250 µg/mL). In 1979, Ohkawa, Ohishi, and Yagi measured lipid peroxide formation by TBARS formation. For this incubation mixture, 0.4 mL will be treated with sodium dodecyl sulphate (8.1%, 0.2 mL), TBA (0.8%, 1.5 mL) and acetic acid (20%, 1.5 mL, pH 3.5). Once the mixture is made to 4.0 mL, it is kept in a water bath at 100 °C for 1 hour. The mixture of n-butanol and pyridine (10:1 v/v) will be added to 1 mL of distilled water after cooling, and then centrifuged at 4000 rpm for 10 minutes. TBARS can be quantified by removing the butanol-pyridine layer and measuring its absorbance at 532 nm[30,31].

3. Results and Discussion

3.1 Identification of Ligand Target in *Capparis grandis*

The target prediction results for the phytoconstituents of *C. grandis* and *L. pungens* show that these molecules interact with a variety of targets, predominantly enzymes like Carbonic anhydrases and Aldose reductase, along with receptors such as GPCRs and kinases. The majority of the targets fall under the enzyme class, indicating potential modulation of metabolic pathways, while GPCRs and kinases suggest involvement in signalling pathways. High probability scores and the presence of known active compounds highlight the therapeutic potential of these plants in addressing diseases like Diabetes and Immunomodulation. The target classes and their corresponding probabilities suggest significant interactions with key proteins involved in disease progression (Figure 1). The *in-silico* network pharmacology results indicate the following findings for *C. grandis* and *L. pungens* in the context of Diabetes and Immunomodulation: For *C. grandis*, MMP13 was identified as a top active target based on the selected criteria, which include target activity,

organism specificity, and mutation considerations. Due to a relatively smaller set of targets for *C. grandis*, the Cytoscape tool was not applicable for further target analysis. For *L. pungens,* multiple targets were identified, including PTGS2, EGFR, PIK3CG, and SYK (Figure 2). Cytoscape was applicable due to a larger number of targets, and SRC was selected as the primary target for further study. Additional key active targets identified for *L. pungens* included CDK1, PARP1, SRC, and BACE1 (Figure 3).

The molecular targets of the bioactive compounds K-3-G, capparisinine, and cappariloside found in *C. grandis* are shown in this Venn diagram, which also shows the genes associated with diabetes. The complex molecular pathophysiology of diabetes is demonstrated by the fact that a large number of targets are unique to the disease. Rather than nonspecific binding, each phytochemical has a distinct array of common targets with genes relevant to diabetes. The highest degree of overlap is seen with K-3-G, suggesting a somewhat stronger association with pathways associated with diabetes. The little overlap between many chemicals in *C. grandis* indicates that they may work in tandem, bolstering the plant's potential as a multi-target therapeutic agent for the treatment of diabetes.

This graphic shows how genes related to immunomodulation and phytochemical targets in *C. grandis* are converging. K-3-G, capparisinine, and cappariloside show striking parallels with diabetes-associated targets, indicating they may be involved in immune modulation; however, there are fewer immunomodulatory targets. It appears that there is a coordinated modulation of immune signalling pathways, possibly through anti-inflammatory

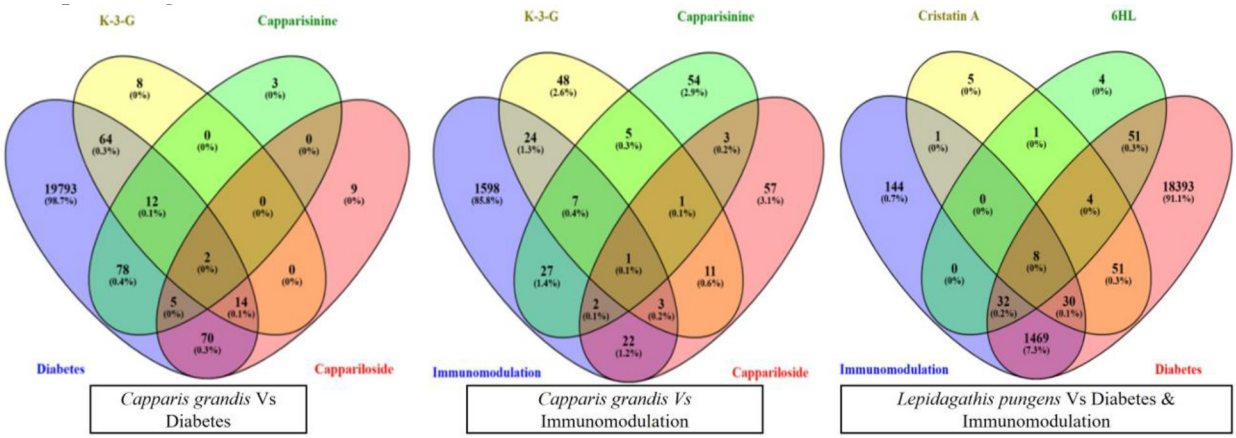

Figure 1. Identification of common targets between disease and selected ligands using Venny Software.

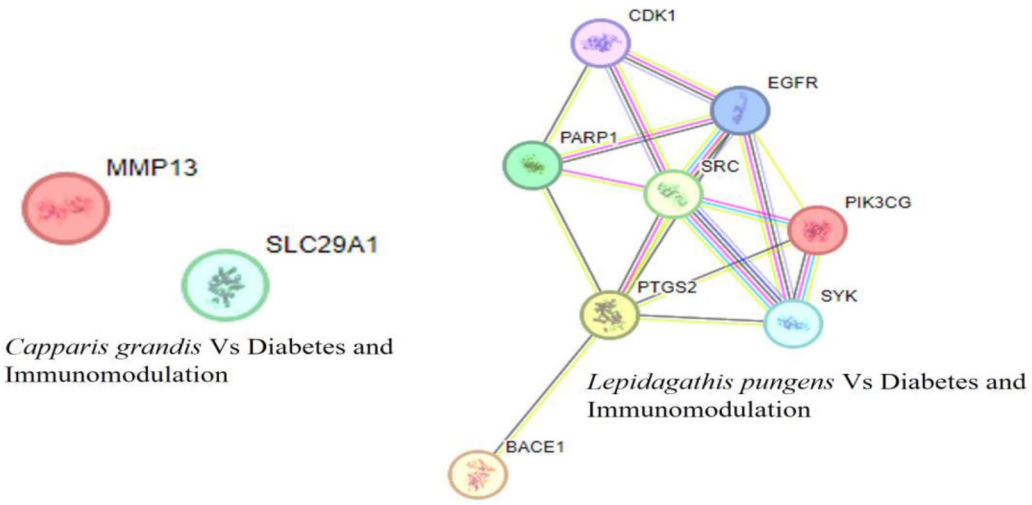

Figure 2. String software enrichment for both plants and disease.

or immuno-regulating mechanisms, as multiple medicines share common targets. *Capparis grandis* may have therapeutic benefits in inflammation-related metabolic disorders, and these results highlight its immunomodulatory importance.

The chemicals Cristatin A and 6HL, which are found in *L. pungens*, have molecular targets that intersect with genes associated with diabetes and immunomodulation, as shown in this Venn diagram. A large number of targets are associated with diabetes, which indicates a great deal of promise as an antidiabetic. Significant shared functions with immunomodulatory genes also point to a dual biological role. There is mounting evidence that *L. pungens* may influence the immuno-inflammatory pathways linked to diabetic complications, thanks to the merging fields of immunomodulation and diabetes. Because of its capacity to address two immune dysfunctions simultaneously, it may be useful as a therapeutic tool in the treatment of diabetes.

3.2 Molecular Docking

The foundation of MolDock is a novel heuristic search technique that combines cavity prediction and differential evolution. A modification of the piecewise linear potential (PLP), the docking scoring function of MolDock incorporates new electrostatic and hydrogen bonding terms. The MolDock Score is a key parameter for analysing the docking results.

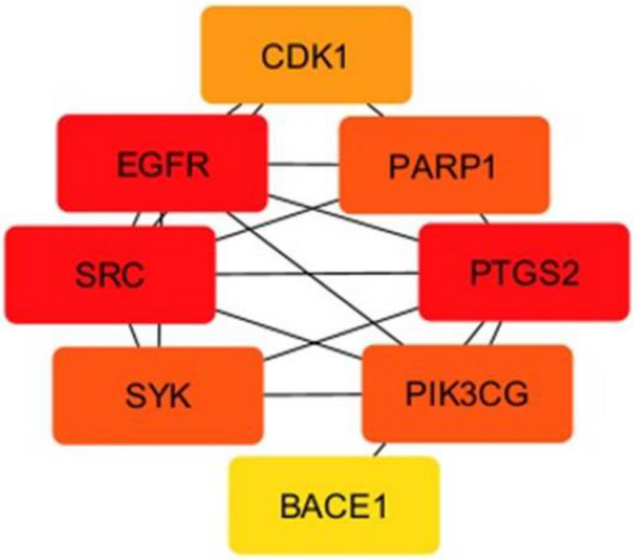

Figure 3. Cytoscape networking for *Lepidagathen pungens.*

MolDock Score, rerank score and hydrogen bond interactions were used for evaluating the ligand molecules. The ligand with the least MolDock score shows a strong affinity towards its target. *In silico* docking analysis of the selected ligands against Diabetes and Immunomodulation is shown in Tables 1-4, respectively.

3.2.1 Phytoconstituents of Lepidagathen pungens vs Diabetes

The docking scores have shown that 636504 (Cristatin-A) is the compound of *Lepidagathen pungens* that has the least MolDock score (-136.94), which means that it has the highest binding affinity to the target protein in comparison to 6-Hydroxyluteolin (-100.795) and the standard drug, Glibenclamide (-126.73). Even though the rerank score of glibenclamide is higher, the overall interaction energy is higher in Cristatin-A than in glibenclamide (-4.07575) and shows better hydrogen bonding (-4.07575) (Table 1). The higher interaction energy of the active site suggests better stability of the latter. Such results indicate that Cristatin-A is a potent natural antidiabetic agent with great potential to exhibit similar or even better binding activity than that of the standard drug, Glibenclamide.

In Figure 4, we can see the molecular docking contacts between the diabetes-associated target protein (PDB ID: 4G0D), the common antidiabetic drug glibenclamide, and two selected phytoconstituents from *L. pungens*, namely Cristain A and Hydroxyluteolin. Highlighting the molecular compatibility and stability of the ligands within the target protein's active site, the image provides a comprehensive illustration of the binding interactions through 2D interaction maps, 3D binding conformations, and secondary structural interactions.

Table 1. Ranking of ligands and poses against Human Collagenase 3 (MMP13) based on MolDock score (Protein: 4G0D)

Ligand	Species Name	MolDock Score	Rerank Score	H Bond
636504	*Lepidagathen pungens* (Cristatin-A)	-136.94	-55.10	-4.07
5281642	*Lepidagathen pungens* (6-Hydroxyluteolin)	-100.79	-85.19	-2.89
3488	Standard Drug (Glibenclamide)	-126.73	-96.56	-1.50

The 2D interaction analysis of Cristatin A reveals persistent binding inside the active site of the target protein, supported by several hydrogen bonds and hydrophobic interactions with essential amino acid residues, namely Gly116(B), Asp117(B), Asn112(B), Asn113(B), Val111(B), and Leu120(A). These interactions demonstrate a strong ligand–protein affinity. The 3D interaction model further confirms that Cristatin A suitably occupies the binding cavity, forming a compact and stable complex strengthened by polar and nonpolar interactions. Analysis of the secondary structure reveals that Cristatin A predominantly engages with β-sheet and loop regions of the protein, indicating little structural distortion and favourable binding orientation, hence endorsing its potential antidiabetic efficacy.

Hydrogen bonds with residues Thr96(B), Thr98(B), Asp99(B), Tyr131(A), Arg95(A), and Trp118(A) are shown in the 2D interaction map, demonstrating that hydroxyluteolin has substantial molecular interactions with the target protein. These interactions indicate strong contributions from electrostatic and π-π stacking. Hydroxyluteolin is shown to be tightly located in the active site, allowing for excellent spatial alignment with key residues, according to the 3D docking visualisation. This protein's enhanced binding stability and functional importance in controlling pathways relevant to diabetes are supported by the secondary structural interaction, which confirms its association with both α-helices and β-sheets.

Glibenclamide, an antidiabetic drug, binds strongly to the target protein, interacting with important residues such as Arg, Tyr131, Asp99, Thr98, and Thrp118 in both molecules. A highly stabilised ligand-protein complex was seen by means of the 3D interaction analysis, which shows that glibenclamide penetrated the binding cavity to a considerable degree. The docking approach is confirmed to be reliable, and a reference benchmark for evaluating the phytoconstituents is provided by the visualisation of secondary structures, which mostly show interactions with β-sheets and helical regions.

All things considered, the docking findings show that the phytoconstituents of *L. pungens*, especially Hydroxyluteolin and Cristatin A, have binding patterns

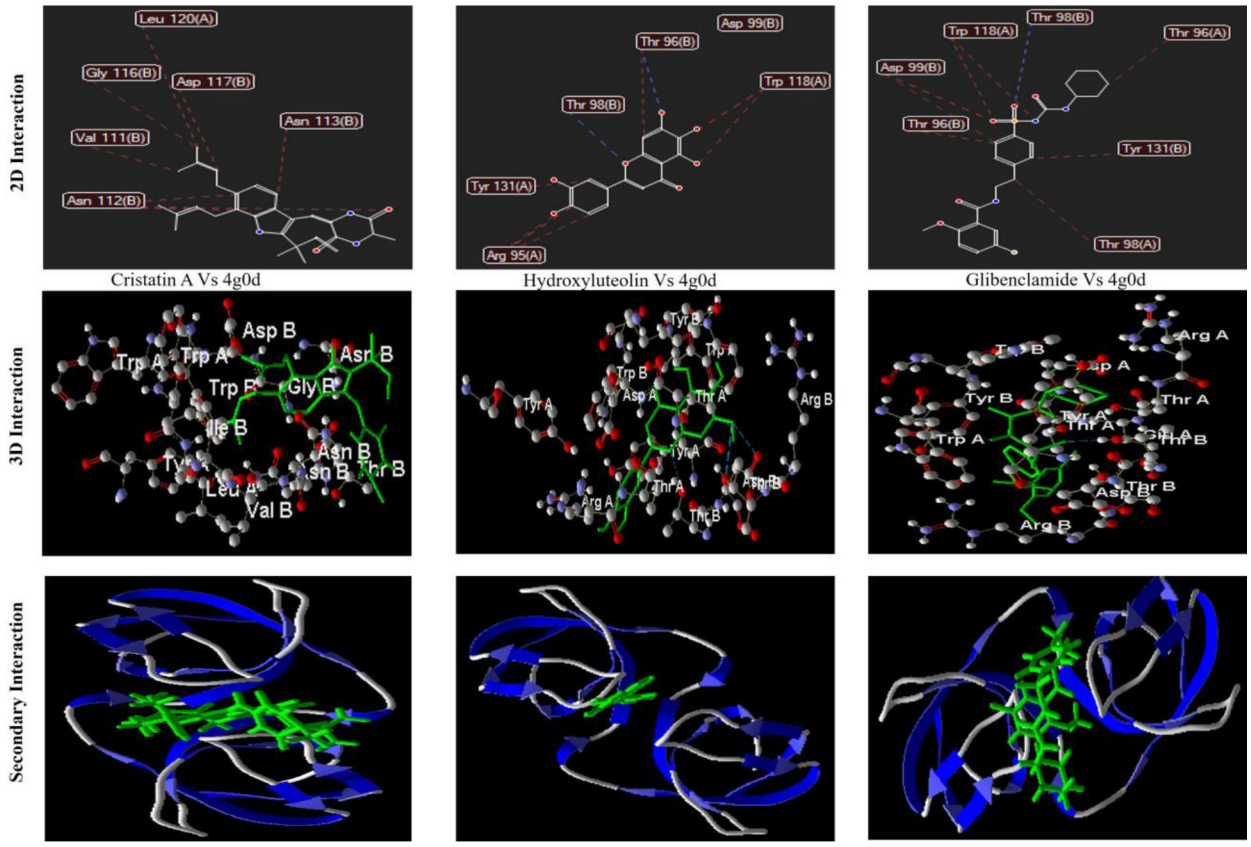

Figure 4. 2D, 3D and secondary interaction of phytoconstituents of *Lepidagathen pungens* against diabetes.

similar to the standard antidiabetic drug glibenclamide. Protein targets associated with diabetes can be efficiently targeted by these compounds because of their strong hydrogen bonding, hydrophobic interactions, and long-lasting secondary structural links. These findings validate the traditional medicinal use of *L. pungens* and provide evidence of its therapeutic value in the treatment of diabetes.

3.2.2 *Phytoconstituents of Capparis grandis vs Diabetes*

The docking results show that of all the *C. grandis* phytochemicals, Cappariloside had the highest MolDock score (-121.784) and a large Rerank score (-71.8133) with a pronounced hydrogen bond interaction (-7.28736), and this implies a high binding affinity (Table 2). Kaempferol-3-Glucoside recorded moderate MolDock (-100.671) and weaker Rerank (-39.9651) scores, but the highest hydrogen bonding (-10.9915), suggesting the possible specific interaction.

Capparisinine was lower in MolDock (-108.137) and moderate in Rerank (-86.6202) with a low level of hydrogen bonding (-2.5). The standard drug was Glibenclamide, and this had a MolDock of -105.163, a high Rerank (-88.927) and a low hydrogen bonding (-0.0379) to act as a control in terms of binding efficiency. In general, Cappariloside seems to be the best candidate.

Through hydrogen bonding and electrostatic interactions with key residues such as Lys276(C), His277(C), Lys279(C), and Asp305(C), the 2D interaction study of capparisinine shows that it binds persistently inside the active site of the diabetes-related protein (4G0D). The presence of these interactions

Table 2. Ranking of ligands and poses against Human Collagenase 3 (MMP13) based on MolDock score (Protein: 4G0D)

Ligand	Species Name	MolDock Score	Rerank Score	H Bond
11972305	*Capparis grandis* (Cappariloside)	-121.78	-71.81	-7.28
5373784	*Capparis grandis* (Capparisinine)	-108.13	-86.62	-2.50
5282102	*Capparis grandis* (Kaempferol-3-Glucoside)	-100.67	-39.96	-10.99
3488	Standard drug (Glibenclamide)	-105.16	-88.92	-0.03

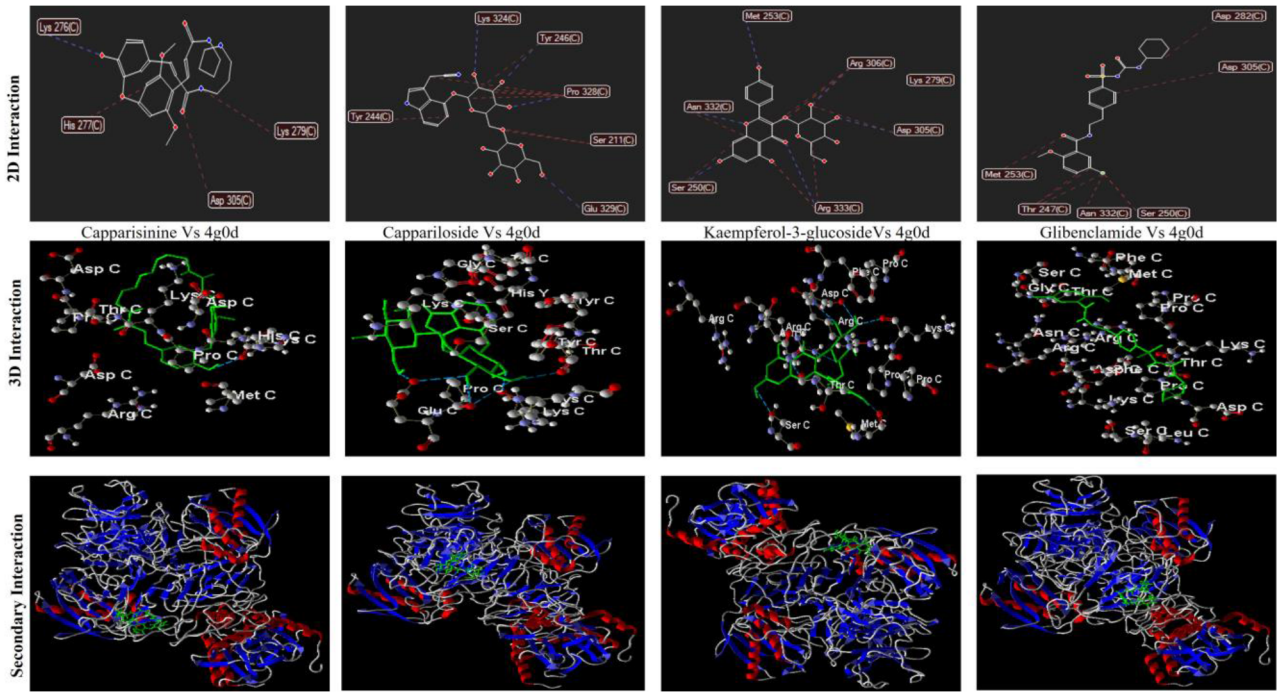

Figure 5. 2D, 3D and secondary interaction of phytoconstituents of *Capparis grandis* against diabetes.

indicates strong polar bonds, which help to stabilise the ligand. Capparisinine successfully fills the binding pocket, forming a tight ligand-protein complex supported by neighbouring amino acid residues, as shown in the 3D interaction picture (Figure 5). The secondary structure analysis shows that the capparisinine mainly interacts with the loop and β-sheet parts of the protein, which means it can be integrated into the protein well without causing major changes in its conformation, which supports its potential as an antidiabetic.

Based on the 2D interaction map, cappariloside forms many hydrogen bond interactions with residues like Tyr244(C), Tyr246(C), Lys324(C), Ser211(C), Pro328(C), and Glu329(C). These interactions show that aromatic and polar residues work together to form a strong ligand affinity. Cappariloside is seen to be well-integrated into the active site in the 3D docking visualisation, creating a thorough interaction network that strengthens the binding. The ligand's potential as an antidiabetic phytoconstituent is highlighted by the secondary structural interaction, which highlights its connection with the protein's α-helical and β-sheet domains and indicates excellent stabilisation of the ligand inside the catalytic pocket.

Strong hydrogen bonding and electrostatic interactions with residues such as Met253(C), Asn332(C), Arg306(C), Arg333(C), Asp305(C), and Ser250(C) are shown in the two-dimensional interaction profile of kaempferol-3-glucoside. Based on these interactions, it appears that charged and polar amino acids form a strong binding pattern. Optimal alignment and interaction with crucial residues are facilitated by the 3D interaction model, which shows that kaempferol-3-glucoside penetrates the active site deeply. The ligand interacts with β-sheets and flexible loop areas, according to secondary structure analysis, which could increase binding stability and biological activity against targets relevant to diabetes.

The interactions between the target protein and the antidiabetic drug glibenclamide and important residues like Met253(C), Thr247(C), Asn332(C), Ser250(C), Asp282(C), and Asp305(C) demonstrate a strong binding affinity for the target protein. Hydrophobic contacts and substantial hydrogen bonding are shown in the two-dimensional interaction map, which supports the idea of effective ligand anchoring. Glibenclamide successfully occupies the binding pocket, as shown by the 3D docking model, creating a stable ligand-protein pair. The docking process is confirmed, and a baseline for comparison with compounds originating from plants is established by analysis of secondary structural interactions, which primarily include α-helices and β-sheets.

Phytoconstituents of *C. grandis*, including capparisinine, cappariloside, and kaempferol-3-glucoside, show strong and consistent interactions with the diabetes-related protein 4G0D, similar to the traditional medicine glibenclamide, according to the docking experiments. They may regulate metabolic processes associated with diabetes because of the abundance of hydrogen bonds, electrostatic interactions, and beneficial secondary structural connections that comprise them. In support of *C. grandis*' traditional use as an antidiabetic, these results provide molecular-level data.

3.2.3 Phytoconstituents of Lepidagathen pungens vs Immunomodulation

The results of molecular docking indicate that the Cristatin-A of *L. pungens* had the highest MolDock score (-125.94), which suggests high overall binding affinity, but the Rerank score (-36.10) was relatively low, implying not such a good optimised binding energy. It had an interaction of moderate hydrogen bond (-5.07). On the other hand, 6-Hydroxyluteolin possessed a lower MolDock score (-102.79) and a higher Rerank score (-68.19) with slightly weaker hydrogen bonding (-4.84), which shows more stable binding in the refined

Table 3. Ranking of ligands and poses against the Intertwined dimer of the c-Src SH3 domain mutant T125S based on MolDock score (Protein: 7a3d)

Ligand	Species Name	MolDock Score	Rerank Score	H Bond
636504	*Lepidagathen pungens* (Cristatin-A)	-125.94	-36.10	-5.07
5281642	*Lepidagathen pungens* (6-Hydroxyluteolin)	-102.79	-68.19	-4.84
2265	Standard Drug (Azathioprine)	-117.40	-80.77	-6.24

pose (Table 3). The conventional drug, Azathioprine, had an intermediate MolDock (-117.40), a high Rerank score (-80.77) and a hydrogen bond (-6.24) and acts as a good reference. All in all, Cristatin-A has shown good binding potential, whereas Azathioprine is highly optimised (Figure 6).

Some phytoconstituents docked with the target protein and bound to it, as seen in the figure. Ribbon representations of protein-ligand complexes (right panel), 2D interaction diagrams (left panel), and 3D visualisations of ligand-protein interactions (middle panel) highlight the binding orientation, important interacting amino acid residues, and stability of the complexes, respectively, and illustrate the results.

The ligand forms many non-covalent interactions inside the target protein's active site, as shown in the two-dimensional interaction diagram. The ligand is stabilised within the binding pocket by hydrophobic interactions with residues like Val and Tyr, and by hydrogen bonds with important residues like Asp, Thr, and Trp. The strong and specific affinity for the catalytic region is shown by these interactions. The ligand's deep positioning within the binding cavity is confirmed by the 3D interaction model. In this compact and thermodynamically favourable combination, the

ligand (green) is surrounded by residues from the active site. To secure the ligand, hydrogen bonding and π-π stacking interactions are necessary. The ligand is shown to be located in the middle of the protein's binding cleft in the ribbon image. The ligand is well-accommodated by the neighbouring **α-helices and β-sheets, suggesting good structural compatibility with little steric hindrance.**

A higher interaction frequency compared to the previous complex is shown by the 2D interaction

map. An enhanced binding affinity is shown by hydrogen bonds with aspartic acid, threonine, and arginine residues, as well as by π-π interactions involving tryptophan residues. There must be a balanced force

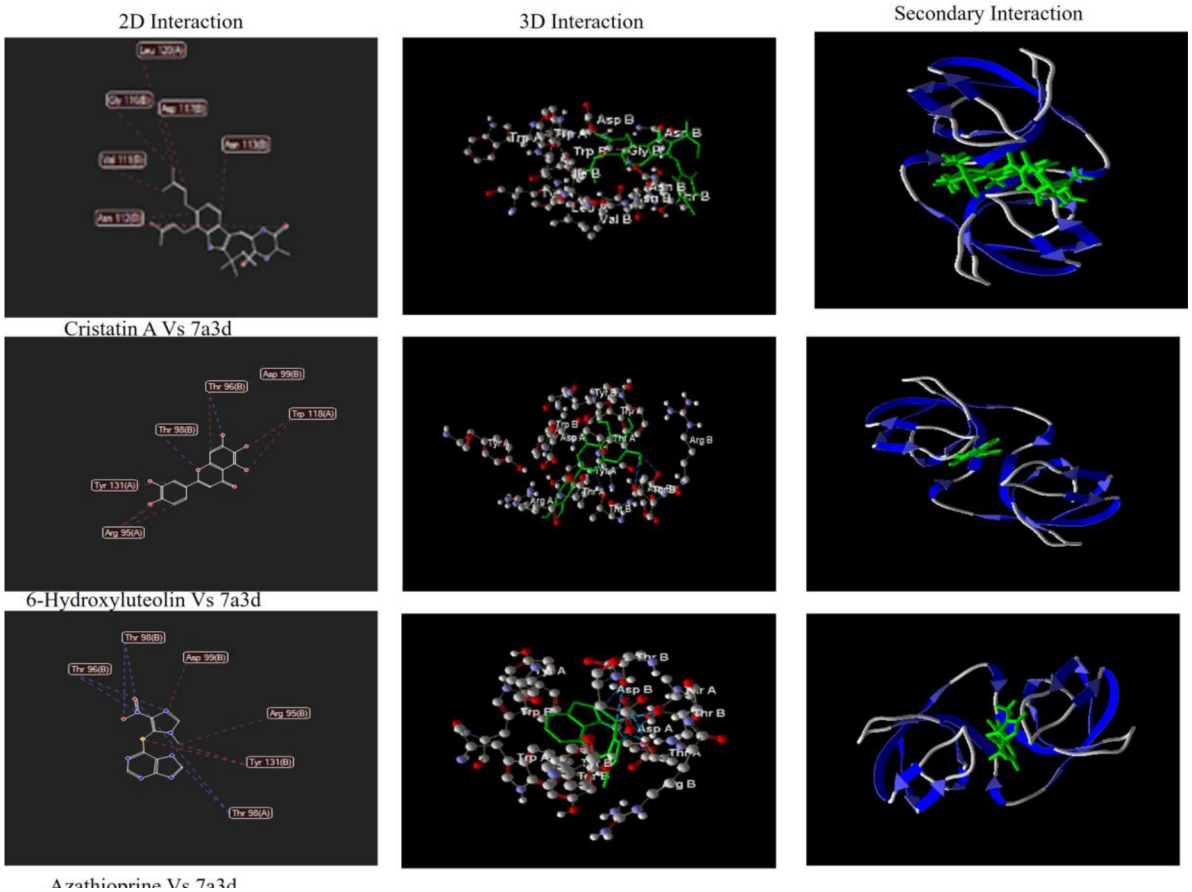

Figure 6. 2D, 3D and secondary interaction of phytoconstituents of *Lepidagathen pungens* against Immunomodulation.

contributing to stability if polar and hydrophobic interactions are present. The three-dimensional model shows the ligand interacting with residues in different parts of the binding pocket at the same time. Docking stability is improved, and inhibitory activity may be indicated by this multi-point attachment, which efficiently obstructs the active site. The ribbon model of the protein-ligand complex shows that the ligand is bound to the protein at certain locations within the binding channel. The likelihood of effective regulation of protein activity is increased by this orientation.

Threonine and aspartate residues form strong hydrogen bonds, while arginine and tyrosine interact hydrophobically, as shown in the two-dimensional interaction map. The ligand is in the perfect position to interfere with substrate binding or catalytic activity, depending on the interaction pattern. The three-dimensional model of the interaction shows a tightly packed ligand-protein complex in which the ligand forms a strong web of interactions. The binding affinity is enhanced due to the probable π-π and van der Waals interactions suggested by the proximity of aromatic residues. It is confirmed by the ribbon structure that the ligand binds steadily to the active site. There is minimal structural strain, and the ligand is in an ideal binding conformation since it is in the middle and supported by nearby secondary structural components.

3.2.4 *Phytoconstituents of Capparis grandis vs Immunomodulation*

The docking outcomes show that Cappariloside had the best MolDock score (-118.71) or the highest overall

Table 4. Ranking of ligands and poses against the Intertwined dimer of the c-Src SH3 domain mutant T125S based on MolDock score (Protein: 7a3d)

Ligand	Species Name	MolDock Score	Rerank Score	H Bond
11972305	*Capparis grandis* (Cappariloside)	-118.71	-68.87	-6.25
5373784	*Capparis grandis* (Capparisinine)	-100.13	-86.41	-2.52
5282102	*Capparis grandis* (Kaempferol-3-Glucoside)	-98.67	-39.87	-10.02
2265	Standard drug (Azathioprine)	-106.18	-76.88	-6.24

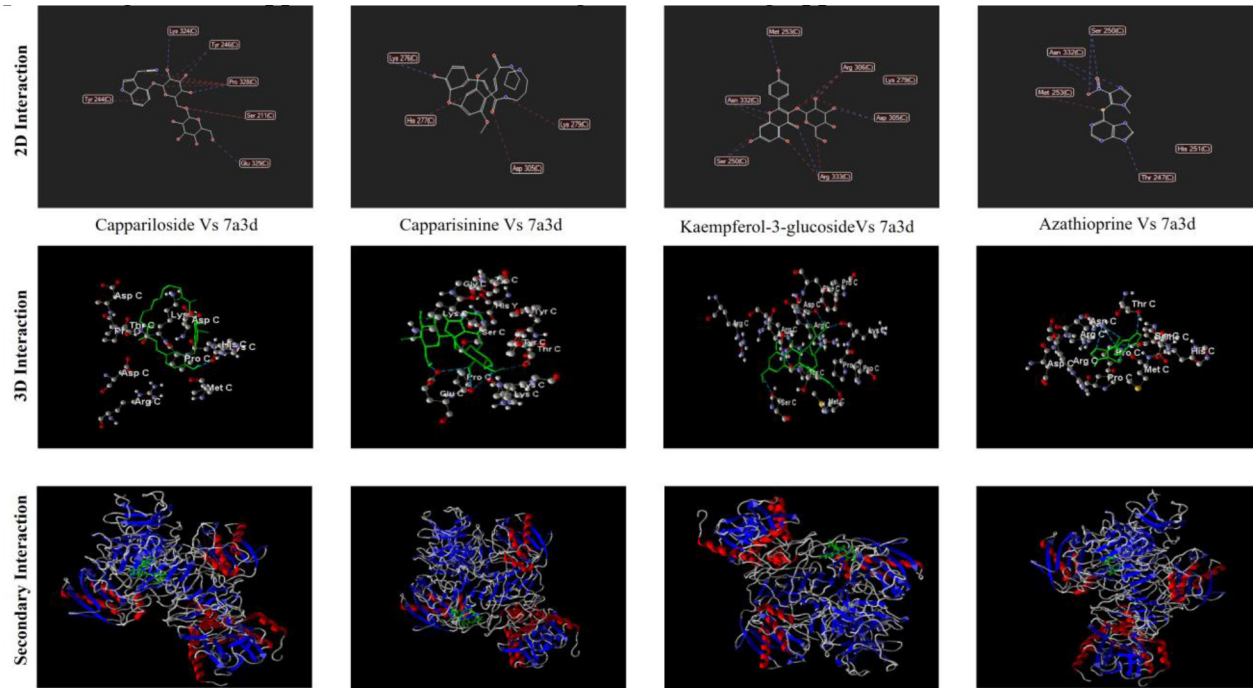

Figure 7. 2D, 3D and secondary interaction of phytoconstituents of *Capparis grandis* against Immunomodulation.

binding affinity, average Rerank score (-68.87), and hydrogen bond interaction (-6.25) of all the compounds of *C. grandis*. At a lower MolDock stage (-100.13) but with higher Rerank (-86.41), Capparisinine has a better binding stability with the disrupted hydrogen bonding (-2.52). Kaempferol-3-Glucoside had the lowest MolDock -98.67 and Rerank -39.87 scores (Table 4), yet it was characterised by strong hydrogen bonds -10.02. There were equal binding parameters with the standard drug Azathioprine (-106.18), which was a good reference point. In general, Cappariloside exhibits the greatest binding opportunities.

The target protein (PDB ID: 7A3D) and the reference drug azathioprine are shown in the molecular docking interactions in the illustration. To provide a comprehensive understanding of binding behaviour and stability, the docking data for each drug are displayed as 2D interaction maps (top row), 3D ligand-protein interaction models (middle row), and secondary structure ribbon representations (bottom row).

Cappariloside forms many electrostatic interactions and hydrogen bonds with amino acid residues such as Lys324, Tyr246, Pro328, Ser211, Glu329, and Tyr244, as seen in the two-dimensional interaction picture. All of these interactions show that the ligand is firmly attached to the active site. Cappariloside (green) is shown to be tightly bound to the binding pocket in the 3D interaction model, with residues like Asp, Lys, His, Pro, Met, and Arg around it. This forms a stable interaction network with hydrogen bonds and polar interactions (Figure 7). Based on the secondary structure representation, cappariloside binds to the protein in a stable and favourable orientation without significantly disrupting its conformation, since it fills the central catalytic cavity and interacts with both α-helical and β-sheet areas.

Capparisinin has a strong ligand-protein affinity in the two-dimensional interaction map by forming hydrophobic interactions and hydrogen bonds with residues such as Lys276, His277, Lys279, Asp305, and Tyr. As can be seen in the three-dimensional model, capparisinin interacts with residues Ser, Tyr, His, Lys, Pro, and Glu, and occupies a prime position within the active site. The binding stability is enhanced when many polar contacts are present. Supporting capparisinin's possible inhibitory activity, the secondary interaction ribbon model shows that it fits well within the binding groove, forming linkages across several secondary structural characteristics. Strong binding inside the active pocket is indicated by the 2D interaction diagram, which shows strong hydrogen bonding interactions with residues including Met253, Asp332, Arg306, Lys279, Asp305, Ser250, and Arg333. The 3D interaction model confirms strong ligand-protein interactions; kaempferol-3-glucoside forms a stable and strong contact network with Arg, Asp, Pro, Ser, Met, and Gly residues. Based on the secondary structure model, the ligand enters the binding cavity and interacts with key protein functional regions, which could hinder substrate availability and protein activity. The 2D interaction map shows that

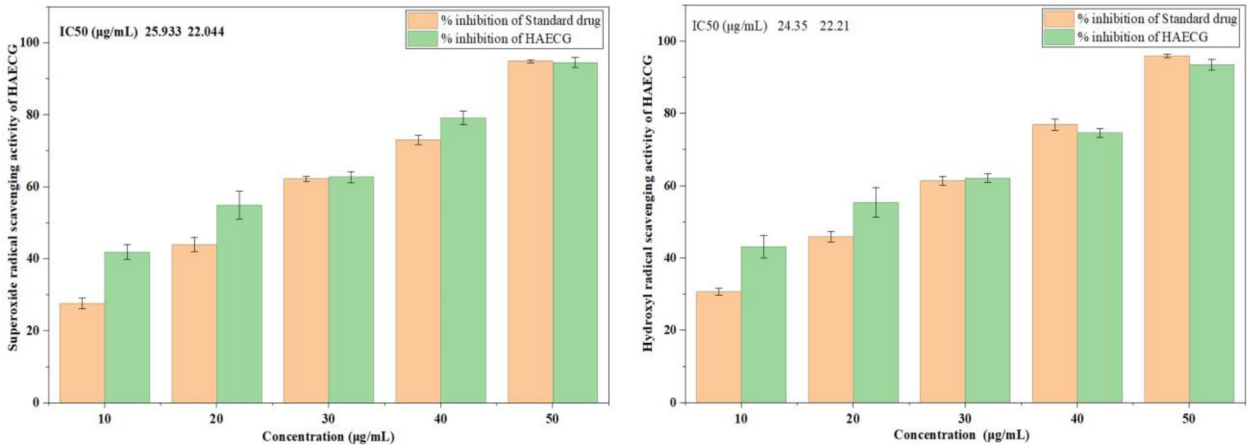

Figure 8. *In vitro* antioxidant activity of HAECG evaluated by superoxide and hydroxyl radical scavenging assays.

azathioprine has moderate binding interactions with residues, primarily hydrogen bonding with Asp332, Met253, Ser250, His251, and Thr247. A lower level of stability within the active site is indicated by the fact that azathioprine displays fewer interactions in the 3D interaction model compared to the phytoconstituents. By reducing its area and attaching to the same binding pocket, azathioprine forms fewer stabilising contacts with neighbouring secondary structural components, as shown by the ribbon model of the secondary structure.

3.3 *In Vitro* Anti-oxidant Activity

Using superoxide radical scavenging and hydroxyl radical scavenging assays at different concentrations (10-50 µg/mL). The data are presented as mean ± standard deviation, and the antioxidant activity is measured as % inhibition.

3.3.1 Superoxide Radical Scavenging Assay

The superoxide radical scavenging assay showed that HAECG's radical scavenging activity was enhanced in a concentration-dependent manner. More inhibition was observed at lower concentrations (10 and 20 µg/mL) of HAECG compared to the conventional medicine, indicating improved early antioxidant effect. Significant scavenging effects were observed at high concentrations (30-50 µg/mL) for both HAECG and the reference drug, with inhibition values approaching saturation. The IC_{50} values support these results; HAECG showed a lower IC_{50} (22.044 µg/mL) compared to the reference drug (25.933 µg/mL), indicating that HAECG is more effective in drawing superoxide radicals at lower doses.

3.3.2 Hydroxyl Radical Scavenging Assay

There was a dose-dependent improvement in the hydroxyl radical scavenging activity (right panel) for both the conventional medicine and HAECG. HAECG showed consistently high inhibitory percentages across all doses examined, with the most pronounced effects at lower doses (Figure 8). The results from the IC_{50} experiment showed that compared to the usual treatment, HAECG had a better ability to scavenge hydroxyl radicals (22.21 µg/mL). It has been found that hydroxyl radicals, which are known to cause substantial oxidative damage to biomolecules, can be more effectively neutralised by HAECG.

HAECG exhibited significant scavenging activity, with the inhibition percentage increasing with concentration. At 50 µg/mL, HAECG showed a

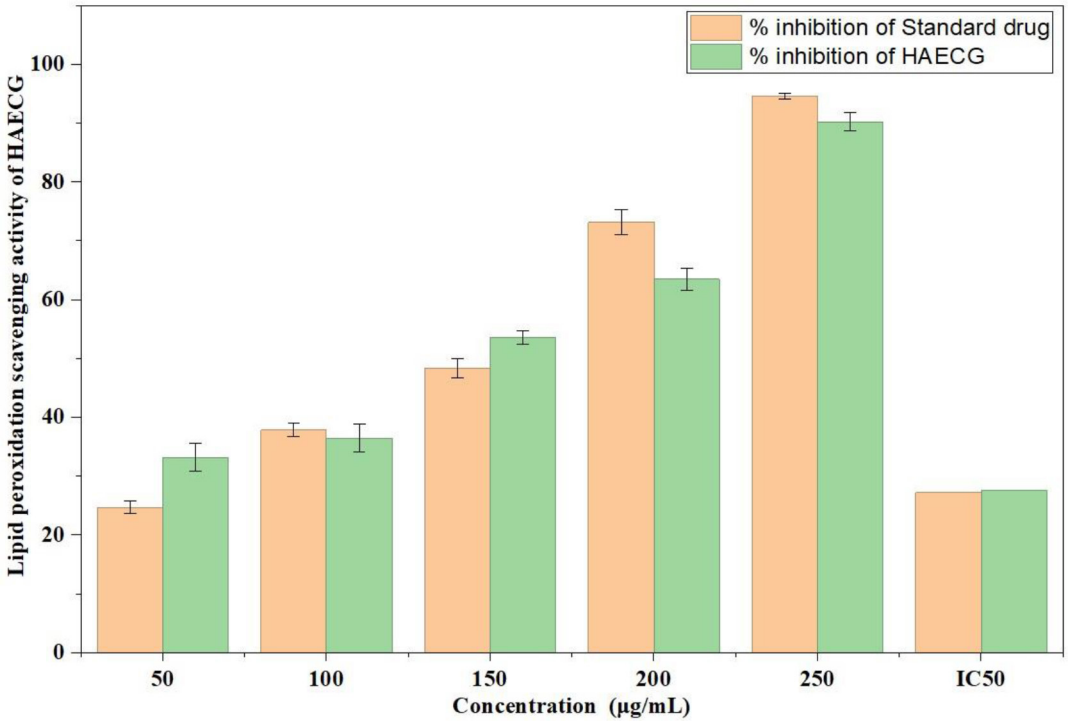

Figure 9. Lipid peroxidation scavenging activity of HAECG in comparison with a standard drug.

94.44% inhibition, comparable to the standard drug, which had 94.86% inhibition. The IC_{50} values for HAECG (22.044 µg/mL) were lower than the standard drug (25.933 µg/mL), indicating superior efficacy in scavenging superoxide radicals. The hydroxyl radical scavenging activity also increased with concentration, with HAECG achieving 93.44% inhibition at 50 µg/mL, which is slightly lower than the standard drug (95.86%). The IC_{50} for HAECG (22.21 µg/mL) (Figure 9) was close to that of the standard drug (24.35 µg/mL), suggesting a strong potential in scavenging hydroxyl radicals. For lipid peroxidation, HAECG demonstrated a dose-dependent increase in inhibition, reaching 90.20% at 250 µg/mL. Although it was lower than the standard drug's 94.59% at the same concentration, HAECG showed an IC_{50} value of 27.618 µg/mL, which is comparable to the standard drug's IC_{50} of 27.22 µg/mL.

Diabetes mellitus is a metabolic disease that is complex and is typified by persistent hyperglycemia because of insulin secretion disorders, insulin action, or a combination of both. The multifactorial characteristic of the disease consists of metabolic dysfunction, immune dysregulation, and this leads to secondary complications like neuropathy, nephropathy and cardiovascular disorders. The shortcomings of synthetic antidiabetic agents, such as adverse effects and target specificity, as noted in the introduction, have led to the study of natural compounds with multi-targeted effects in spite of their limitations. Medicinal plant phytochemicals have diverse actions, including the improvement of insulin sensitivity and secretion, regulation of inflammatory and immune response, and are promising drugs of the future. The molecular docking assay carried out shed light on the correlation between phytochemical structure and affinity with diabetic and immunomodulatory targets. The high MolDock and hydrogen bond scores of Cristatin-A and Cappariloside emphasise the possibility of using them as dual modulators in the treatment of diabetes, both in their application to glucose metabolism and in the related pathways of inflammation. The MolDock score of Cristatin-A of *L. pungens* indicated an exceptionally low affinity against MMP-13 (-136.94), indicating a stronger interaction of the compound with the antidiabetic drug than with the standard antidiabetic drug Glibenclamide (-126.73). Its polypeptide structure with numerous hydrogen bonds and fixed patterns of interaction suggests that it is incredibly fit to occupy the active site of the enzyme, which may help to inhibit collagenase activity: a process associated with disorders of diabetics, such as tissue degeneration and poor wound healing.

Correspondingly, *C. grandis* Cappariloside exhibited high binding energy (-121.78) and high hydrogen bond formation (-7.28) to MMP-13, which is better than Glibenclamide. This indicates that it could adjust glucose homeostasis and oxidative stress. Although it exhibited a higher hydrogen bonding, kaempferol-3-glucoside had lower MolDock scores, which suggests that the stability of the ligand-protein interaction is determined by ideal energy balance, rather than by bond formation. Cristatin-A was found to be the most active ligand against (-125.94) in the analysis of immunomodulatory activity against c-Src SH3 domain compared to a standard Azathioprine (-117.40). This means that it has the capacity to affect the immune signalling pathways that may be of significance in the autoimmune-mediated injuries to the β-cells. Cappariloside (-118.71) showed a high level of binding affinity with similar hydrogen bonding to the Azathioprine and indicated that it has the capacity to control immune responses in chronic inflammatory processes and insulin resistance. The stability of these phytoconstituents in the two plants promotes their scope of application in therapy. Their various hydrogen binding profiles and the preferred binding conformations of the receptors suggest high receptor compatibility, which is associated with previous studies that attribute immunomodulatory and antidiabetic effects to flavonoids and glycosides. Metabolic and immune bifunctional targeting is a supportive solution to the treatment of diabetes, which conventional single-pathway drugs fail to do. Thus, the results prove the ethnopharmacological applicability of *L. pungens* and *C. grandis* and those to be an outline for further *in vitro* and *in vivo* validation in the development of new phytopharmaceutical preparations.

4. Conclusion

In silico results show that the bioactive compounds of *L. pungens* and *C. grandis* have a high binding affinity with diabetic (MMP-13) and immunomodulatory (c-Src SH3)

targets. The most promising ligands were cristatin-A and cappariloside, which outperformed common drugs in MolDock and hydrogen bond parameters, namely Glibenclamide and Azathioprine. The ability to maintain a stable interaction with the active sites of both proteins indicates the dual therapeutic potential, namely, enhancing glucose metabolism by regulating the immune reactions involved in the development of diabetes. These findings demonstrate the synergistic pharmacological nature of these medicinal plants, which strengthens their traditional use and the possible use of these medicinal plants in the design of plant-based anti-diabetic agents. These computational observations should be met with further biochemical and pharmacological research to verify these observations and understand the exact mechanisms of action.

5. Acknowledgement

The authors would like to express their gratitude to the Department of Pharmaceutical Chemistry, School of Pharmaceutical Sciences, VISTAS, Pallavaram, Chennai, Tamil Nadu, Chennai 600117, Tamil Nadu, India, for their support and encouragement during the preparation and submission of this article.

6. References

1. Alam S, Sarker MM, Sultana TN, Chowdhury MN, Rashid MA, Chaity NI, Zhao C, Xiao J, Hafez EE, Khan SA, Mohamed IN. Antidiabetic phytochemicals from medicinal plants: prospective candidates for new drug discovery and development. **Front Endocrinol. 2022**; 13:800714. https://doi.org/10.3389/fendo.2022.800714 PMid: 35282429 PMCid: PMC8907382.
2. Cardoso FC, de Carvalho FE, de Freitas TF, Rezende B, Coelho MG, Montes GC, Martins RC. Antinociceptive in vivo activity and chemical profiling by UHPLC-MS/MS of stem bark and leaves extracts of *Ficus maxima* Mill. (*Moraceae*). **J Ethnopharmacol. 2025**; 337:118793. https://doi.org/10.1016/j.jep.2024.118793 PMid: 39251148.
3. American Diabetes Association. Diagnosis and classification of diabetes mellitus. **Diabetes Care. 2010**; 33(Suppl 1):S62-S69. https://doi.org/10.2337/dc10-S062 PMid: 20042775 PMCid: PMC2797383.
4. Benzie IF, Strain JJ. The ferric reducing ability of plasma (FRAP) as a measure of antioxidant power: the FRAP assay. **Anal Biochem. 1996**; 239(1):70-76. https://doi.org/10.1006/abio.1996.0292 PMid: 8660627.
5. Chen M, Yang J, Tang C, Lu X, Wei Z, Liu Y, Yu P, Li H. Improving ADMET prediction accuracy for candidate drugs: factors to consider in QSPR modeling approaches. **Curr Top Med Chem. 2024**; 24(3):222-242. https://doi.org/10.2174/0115680266280005231207105900 PMid: 38083894.
6. Dahmoune F, Nayak B, Moussi K, Remini H, Madani K. Optimization of microwave-assisted extraction of polyphenols from *Myrtus communis* L. leaves. **Food Chem. 2015**; 166:585-595. https://doi.org/10.1016/j.foodchem.2014.06.066 PMid: 25053097.
7. García-Gurrola A, Martínez AL, Wall-Medrano A, Olivas-Aguirre FJ, Ochoa-Ruiz E, Escobar-Puentes AA. Phytochemistry, anti-cancer, and anti-diabetic properties of plant-based foods from Mexican agrobiodiversity: A review. **Foods. 2024**; 13(24):4176. https://doi.org/10.3390/foods13244176 PMid: 39767118 PMCid: PMC11675762.
8. Giri B, Dey S, Das T, Sarkar M, Banerjee J, Dash SK. Chronic hyperglycemia mediated physiological alteration and metabolic distortion leads to organ dysfunction, infection, cancer progression and other pathophysiological consequences: An update on glucose toxicity. **Biomed Pharmacother. 2018**; 107:306-328. https://doi.org/10.1016/j.biopha.2018.07.157 PMid: 30098549.
9. He D, Cui C. Plant heteropolysaccharides as potential anti-diabetic agents: A review. **Curr Issues Mol Biol. 2025**; 47(7):533. https://doi.org/10.3390/cimb47070533 PMid: 40729002 PMCid: PMC12294070.
10. Kar S, Roy K, Leszczynski J. Impact of pharmaceuticals on the environment: risk assessment using QSAR modeling approach. **Comput Toxicol Methods Protoc. 2018**: pp. 395-443. https://doi.org/10.1007/978-1-4939-7899-1_19 PMid: 29934904 PMCid: PMC7120680.
11. Kim S, Thiessen PA, Bolton EE, Chen J, Fu G, Gindulyte A, Han L, He J, He S, Shoemaker BA, Wang J. PubChem substance and compound databases. **Nucleic Acids Res. 2016**; 44(D1):D1202-D1213. https://doi.org/10.1093/nar/gkv951 PMid: 26400175 PMCid: PMC4702940.
12. Li J, Liu J, Shi W, Guo J. Role and molecular mechanism of *Salvia miltiorrhiza* associated with chemical compounds in the treatment of diabetes mellitus and its complications: a review. **Medicine (Baltimore). 2024**; 103(16):e37844. https://doi.org/10.1097/MD.0000000000037844 PMid: 38640337 PMCid: PMC11029945.
13. Lodge JA, Maier T, Liebl W, Hoffmann V, Sträter N. Crystal structure of *Thermotoga maritima* α-glucosidase AglA defines a new clan of NAD+-dependent glycosidases. **J Biol Chem. 2003**; 278(21):19151-19158. https://doi.org/10.1074/jbc.M211626200 PMid: 12588867.
14. Marinova G, Batchvarov V. Evaluation of the methods for determination of the free radical scavenging activity by DPPH. **Bulg J Agric Sci. 2011**; 17(1):11-24.

15. Na MK, An RB, Jin WY, Min BS, Yoo JK, Kim YH, Bae KH. Antioxidant effects of plant extracts on free radicals and lipid peroxidation. **Nat Prod Sci. 2003**; 9(4):226-231.
16. Olufolabo KO, Lüersen K, Oguntimehin SA, Nchiozem-Ngnitedem VA, Agbebi EA, Faloye KO, Nyamboki DK, Rimbach G, Matasyoh JC, Schmidt B, Moody JO. *In vitro* and *in silico* studies reveal antidiabetic properties of arylbenzofurans from the root bark of *Morus mesozygia* Stapf. **Front Pharmacol. 2024**; 15:1338333. https://doi.org/10.3389/fphar.2024.1338333 PMid: 38482058 PMCid: PMC10935558.
17. Ogurtsova K, Guariguata L, Barengo NC, Ruiz PL, Sacre JW, Karuranga S, Sun H, Boyko EJ, Magliano DJ. IDF diabetes Atlas: global estimates of undiagnosed diabetes in adults for 2021. **Diabetes Res Clin Pract. 2022**; 183:109118. https://doi.org/10.1016/j.diabres.2021.109118 PMid: 34883189.
18. Patel DK, Kumar R, Laloo D, Hemalatha S. Natural medicines from plant source used for therapy of diabetes mellitus: An overview of its pharmacological aspects. **Asian Pac J Trop Dis. 2012**; 2(3):239-250. https://doi.org/10.1016/S2222-1808(12)60054-1
19. Phoopha S, Sangkaew S, Wattanapiromsakul C, Nuankaew W, Kang TH, Dej-Adisai S. Phytochemical investigation of *Lepionurus sylvestris* Blume and their anti-diabetes effects via anti-alpha glucosidase and insulin secretagogue activities plus molecular docking. **Pharmaceuticals. 2023**; 16(8):1132. https://doi.org/10.3390/ph16081132 PMid: 37631052 PMCid: PMC10458858.
20. Pillai MG, Antony H. Harnessing the immunomodulatory potential of natural products in precision medicine: A comprehensive review. **Explor Drug Sci. 2024**; 2(3):339-360. https://doi.org/10.37349/eds.2024.00050
21. Prabhakar P, Mukherjee S, Kumar A, Rout RK, Kumar S, Verma DK, Dhara S, Rao PS, Maiti MK, Banerjee M. *In silico, in vitro* and *ex vivo* evaluation of the antihyperglycaemic, antioxidant and cytotoxic properties of *Coccinia grandis* L. leaf extract. **Food Technol Biotechnol. 2024**; 62(2):188-204. https://doi.org/10.17113/ftb.62.02.24.8162 PMid: 39045303 PMCid: PMC11261651.
22. Prabhakar P, Banerjee M. Antidiabetic phytochemicals: A comprehensive review on opportunities and challenges in targeted therapy for herbal drug development. **Int J Pharm Res. 2020**; Supplementary Issue 1:1673. https://doi.org/10.31838/ijpr/2020.SP1.242
23. Poovitha S, Parani M. *In vitro* and *in vivo* α-amylase and α-glucosidase inhibiting activities of the protein extracts from two varieties of bitter gourd (*Momordica charantia* L.). **BMC Complement Altern Med. 2016**; 16(Suppl 1):185. https://doi.org/10.1186/s12906-016-1085-1 PMid: 27454418 PMCid: PMC4959359.
24. Pulbutr P, Saweeram N, Ittisan T, Intrama H, Jaruchotikamol A, Cushnie B. *In vitro* α-amylase and α-glucosidase inhibitory activities of *Coccinia grandis* aqueous leaf and stem extracts. J Biol Sci. 2017; 17(2):61-68. https://doi.org/10.3923/jbs.2017.61.68
25. Sasidharan S, Chen Y, Saravanan D, Sundram KM, Latha LY. Extraction, isolation and characterization of bioactive compounds from plant extracts. **Afr J Tradit Complement Altern Med. 2011**; 8(1). https://doi.org/10.4314/ajtcam.v8i1.60483
26. Tan TC, Mijts BN, Swaminathan K, Patel BK, Divne C. Crystal structure of the polyextremophilic α-amylase AmyB from *Halothermothrix orenii*. **J Mol Biol. 2008**; 378(4):852-870. https://doi.org/10.1016/j.jmb.2008.02.041 PMid: 18387632.
27. Tkaczyk A, Bownik A, Dudka J, Kowal K, Ślaska B. *Daphnia magna* model in the toxicity assessment of pharmaceuticals: A review. **Sci Total Environ. 2021**; 763:143038. https://doi.org/10.1016/j.scitotenv.2020.143038 PMid: 33127157.
28. Velmurugan S, Seshai S, Ramachandiran VJ, Reshma A, Anbazhagan S, Vadivel SA. A comprehensive review on phytochemicals with anti-diabetic activity: mechanisms and applications. **J Popul Ther Clin Pharmacol. 2025**; 30:1451-1471. https://doi.org/10.53555/hqaw2e18
29. Wang K, Dong Y, Zhao X, Duan K, Zhao R, Ye Y, Guo J, Pan H, Tang H, Ma Y. Sensitive and rapid sensing of dimetridazole. **J Mol Struct. 2023**; 1284:135458. https://doi.org/10.1016/j.molstruc.2023.135458
30. Wu H, Dushenkov S, Ho CT, Sang S. Novel acetylated flavonoid glycosides from the leaves of *Allium ursinum*. **Food Chem. 2009**; 115(2):592-595. https://doi.org/10.1016/j.foodchem.2008.12.058
31. Zhang Z, Gao Q, Li S, Zeng Z, Zhang Y. Effect of herbal medicine compound promotes beta cell function among type 2 diabetes (T2D) adults. **Contemp Clin Trials Commun. 2023**; 35:101166. https://doi.org/10.1016/j.conctc.2023.101166 PMid: 37520328 PMCid: PMC10372378.

Author Contribution

Conceptualisation: C. Nagamani, P. Balaji; Methodology: C. Nagamani; Software: P. Balaji; Validation: C. Nagamani, P. Balaji; Formal Analysis: C. Nagamani; Investigation: C. Nagamani; Resources: C. Nagamani; Data Curation: C. Nagamani; Writing Original Draft Preparation: C. Nagamani; Writing Review and Editing: P. Balaji; Visualisation: P. Balaji; Supervision: P. Balaji. All authors have read and agreed to the published version of the manuscript.